Few-Body Syst (2024) 65:43
https://doi.org/10.1007/s00601-024-01916-2

Alexander Volya · **Vladimir Zelevinsky**

Puzzles of Exotic Decay Processes

Received: 1 March 2024 / Accepted: 19 March 2024 / Published online: 13 April 2024

Abstract The growing interest in the physics of unstable nuclei, along with their manifestations in laboratory experiments and astrophysical observations, highlights the existence of features in decay processes within complex quantum systems that are not yet fully understood. This paper considers examples of such phenomena, including two-step decay processes, resonance effects, threshold peculiarities, and the interactions between bound and continuum states, as well as the related dynamics.

1 Introduction

Among many-body quantum processes, the spontaneous decay of unstable systems occupies a special place being one of the most fundamental phenomena of quantum dynamics. An active area of current research targets the physics of unstable nuclei observed in the laboratory and in astrophysical data. In the simplest standard description, the decay probability is characterized by the exponential time behavior with the mean life time τ of the initial system or equivalently by the complex energy $E - (i/2)\Gamma$, where $\Gamma = \hbar/\tau$ defines the width of the energy distribution in the non-stationary initial quantum state. Earlier we have discussed non-exponential effects in quantum decays [1] which are hard to observe experimentally [2].

Experimental studies of various decay processes such as sequential and multi-nucleon decays, as presented in Refs. [3–6], pose significant challenges to theoretical understanding of nuclear dynamics at the brink of stability. Combining the complex many-body nuclear structure with the mechanisms of decay and dynamics in the contnuum proves to be a formidable endeavor. Recent attempts to bridge these aspects are documented in References [7–10].

In this paper, we explore some fundamental characteristics of the decay processes, the intricate relationships between nuclear structure and reaction dynamics, the sequential decay mechanisms, and the nuances of the three-body breakup phenomena.

A. Volya (✉)
Department of Physics, Florida State University, Tallahassee, Florida 32306, USA
E-mail: avolya@fsu.edu

V. Zelevinsky
Department of Physics and Astronomy and Facility for Rare Isotope Beams, Michigan State University, East Lansing, Michigan 48824, USA

2 Decay and Resonances

The partial decay width for the transition $1 \xrightarrow{\epsilon} 2$, associated with the corresponding amplitude $A(\epsilon)$, is determined by the Fermi Golden Rule,

$$d\Gamma_{1,2}(\epsilon) = 2\pi \left|A_{1,2}(\epsilon)\right|^2 \delta(E_1 - E_2 - \epsilon)\, d\epsilon; \tag{1}$$

the partial decay width, $d\Gamma_{1,2}(\epsilon)$, is proportional to the square of the amplitude $A_{1,2}(\epsilon)$, under condition of the energy conservation given by the delta function $\delta(E_1 - E_2 - \epsilon)$. This leads to the decay width expressed as a function of the energy difference $\epsilon = E_1 - E_2$,

$$\Gamma_{1,2}(\epsilon) = 2\pi \left|A_{1,2}(\epsilon)\right|^2. \tag{2}$$

The convenient way to a consistent description of the decay processes in terms of the amplitudes $A_{1,2}$ coupling the internal dynamics with continuum channels can be based on the Feshbach projection formalism [11,12]. The detailed introduction to the Feshbach projection formalism and its various applications, including the processes of the quantum signal propagation through periodic structures, can be found in the recent book *Mesoscopic Nuclear Physics* [13]. Further select applications of this formalism can be found in Refs. [8,14–16].

The amplitude for a sequential two-body decay process, where an initial state 1 decays through an intermediate state 2 to a final state 3, denoted as $1 \xrightarrow{\epsilon_1} 2 \xrightarrow{\epsilon_2} 3$, can be expressed as:

$$A_{1,2,3}(\epsilon_1, \epsilon_2) = \frac{A_1(\epsilon_1) A_2(\epsilon_2)}{\epsilon_2 - \left(E_2 - \frac{i}{2}\Gamma_{2,3}(\epsilon_2)\right)}. \tag{3}$$

In this expression, we adopt an on-shell condition formulated as $E_1 = \epsilon_1 + \epsilon_2 + E_3$ and assume that the decay width of the intermediate state, $\Gamma_{2,3}(\epsilon_2)$, is governed exclusively by the decay $2 \xrightarrow{\epsilon_2} 3$.

According to the Fermi Golden Rule, the partial decay width distribution for this sequential decay mechanism is given by:

$$\frac{d\Gamma(E)}{d\epsilon_1 d\epsilon_2} = 2\pi\delta(E - \epsilon_1 - \epsilon_2) \left|A_T(\epsilon_1, \epsilon_2)\right|^2. \tag{4}$$

Here, the total amplitude A_T in eq. (4) encompasses contributions from all possible intermediate states; it must be appropriately (anti)symmetrized to account for identical particles in the final states. In Fig. 1 we illustrate eq. (4) by the integrated result expressing the decay width $\Gamma_{1,2,3}$ of the initial state 1 that is subject to a sequential decay process, namely the intermediate product state 2 further decays into 3, and compare it with the case of a single-step decay width $\Gamma_{1,2}$ where final state 2 is completely stationary. The energy scale here is picked so that $E_1 = 1$ and we set the threshold $E_3 = 0$. The decay widths are shown as a function of the intermediate state energy E_2. The figure also assumes that both decays are governed by a power law phase space scaling $\epsilon^{5/2}$ which represents d-wave decay of a neutral particle. When $E_2 < 1$, the direct decay $1 \to 2$ is open and the instability of the intermediate state 2 does not play much role, note that the plot is logarithmic. The sequential nature of the process is only relevant near threshold when the width of the state 2 is large and overlaps with threshold at $E_2 = 1$ (shown by the dashed vertical line). Above threshold, $E_2 > 1$, only virtual decay is possible, the width becomes exponentially small. The decays of this virtual nature, however, are extremely important in many situations including such as the two-neutron decay in ^{26}O [17], ^{16}Be [3], ^{13}Li [18], exotic proton emitters such as ^{9}N [19], ^{6}Be [20], double beta decays, and many more. As nuclei with significant proton-neutron imbalance are discovered and studied the beta-delayed particle and multi-particle decays are becoming of interest and we discuss one of those cases, ^{11}Be, later in this work.

The behavior seen in Fig. 1 is generally the same in all cases with exception of the s-wave when the state is virtual, see also Ref. [21]. Assuming for brevity one-body channels identified by momentum, the situation is best addressed by reviewing the scattering problem in the complex momentum plane as illustrated in Fig. 2, see pedagogical discussions in Refs. [22–24]. In Fig. 2, the points show various types of singularities that could be encountered in the complex momentum plane (disregarding symmetries): 1 - bound state, 2 - narrow resonance, 3 - broad resonance, 4 - virtual state, and 5 - we refer to as background scattering features. The effect of these singularities on the time evolution of a state is illustrated in Ref. [1]. Integration over the real momentum scattering states $k > 0$ can be replaced through Cauchy's integral formula considering a contour integral shown in figure with the red dashed line, resulting in the pole contributions (2 and 3) that result in the

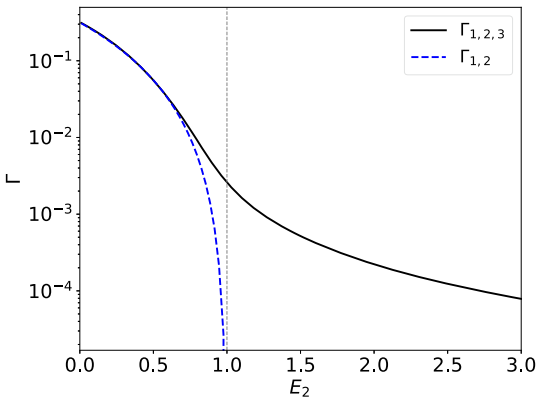

Fig. 1 The decay width (inverse mean lifetime) of the state 1 as a function of the position of the intermediate state 2 relative to the state 3 taken to be at zero energy. The unit of energy is defined so that $E_1 = 1$ and $E_3 = 0$. The two curves compare direct decay, where an intermediate state 2 is considered as stationary, and sequential decay where an intermediate state is a resonance

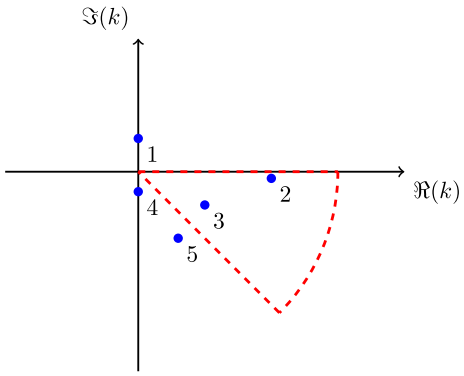

Fig. 2 Types of singularities in the complex momentum plane

exponential decay and "background" provided by the integral along a 45° line. Assuming in simplified units energy $\epsilon = k^2$, the "background" integral over the evolution operator $e^{-i\epsilon t}$ is real and of Gaussian type. This highlights an important destination of virtual states (4) and other scattering features (5) as they never produce an exponentially decaying state. Nevertheless, scattering features because of near-threshold kinematics can result in resonant-like peaks.

The phase space volume plays a major role in determining decay rates, particularly at low energies where it leads to the energy-dependent power law $\Gamma(\epsilon) \propto \epsilon^{\beta}$, as discussed in Refs. [8,10]. From the above discussion $\beta = 1$ represents a critical case when real and imaginary parts of the complex momentum are proportional and can follow the 45° line above or below.

Below we comment on the scaling parameter β across various processes concentrating on the s-wave three-body breakup with neutral particles. For a one-body phase space, the scaling parameter β assumes a value of 1/2 in the case of the s-wave (symmetric) decay. Following the known description [25],

$$\Gamma_1(\epsilon) = \frac{2\hbar^2}{\mu_1 R_1} k, \tag{5}$$

where R_1 is the channel radius parameter for the decay from the resonance 1, the decay width for the s-wave process is proportional to $\sqrt{\epsilon}$, and the leading term in the denominator is of the form of the scattering amplitude (3) in the effective range expansion,

$$\epsilon_2 - \left(E_2 - \frac{i}{2}\Gamma_2(\epsilon_2)\right) \approx \frac{\hbar^2}{\mu_2 R_2}\left(\frac{1}{a_2} + ik_2\right). \tag{6}$$

This behavior is described by the scattering length a_2 of an intermediate state 2 or, equivalently, by the energy parameter ε_2,

$$a_2 = \frac{\Gamma_2(\epsilon)}{2kE_2} = \frac{\hbar^2}{\mu_2 R_2 E_2}, \quad \varepsilon_2 \equiv \frac{\hbar^2}{2\mu_2 a_2^2}. \tag{7}$$

Expression (6) shows that $\beta = 1/2$ leads to a virtual state or bound state, depending on the sign of the scattering length, since the singularity emerges for a pure imaginary momentum.

Addressing the sequential decay with distinguishable particles, we obtain

$$\frac{d\Gamma_{1,2,3}(\epsilon_1, \epsilon_2)}{d\epsilon_2} = \frac{2\lambda}{\pi} \frac{\sqrt{(E_1 - \epsilon_2)\epsilon_2}}{\varepsilon_2 + \epsilon_2}, \tag{8}$$

where

$$\lambda = \frac{R_2}{R_1}\sqrt{\frac{\mu_2}{\mu_1}} \tag{9}$$

is a dimensionless parameter expected to be close to unity. The integrated decay width as a function of the resonance energy E_1 is

$$\Gamma_{1,2,3}(E_1) = \lambda \left[2\varepsilon_2 + E_1 - 2\sqrt{\varepsilon_2(E_1 + \varepsilon_2)}\right]. \tag{10}$$

In contrast, the two-body phase space exhibits a quadratic scaling with energy, $\beta = 2$, attributable to the energy dependence of the integral

$$\int d^3k_1\, d^3k_2 \delta(E - \epsilon_1 - \epsilon_2) \propto E^2. \tag{11}$$

This is evident at very low energies, where $E_1 \ll \varepsilon_2$, leading to the approximation

$$\Gamma_{1,2,3}(E_1) \simeq \lambda \frac{E_1^2}{4\varepsilon_2}. \tag{12}$$

In the opposite regime, when $E_1 \gg \varepsilon_2$, or at higher energies, the decay width simplifies to $\Gamma_{1,2,3}(E_1) \simeq \lambda\, E_1$, setting $\beta = 1$. This distinct scaling behavior underscores the departure from sequential decay processes characterized by a scaling parameter of $\beta = 1/2$.

For identical particles, the total amplitude is given by $A_T^{\pm}(\epsilon_1, \epsilon_2) = \left[A_{1,2,3}(\epsilon_1, \epsilon_2) \pm A_{1,2,3}(\epsilon_2, \epsilon_1)\right]/\sqrt{2}$. In the high energy limit, $E_1 \gg \varepsilon_2$, similarly to the non-identical case, we find $\beta = 1$:

$$\Gamma^{\pm}_{1,2,3}(E_1) \simeq \frac{\pi \pm 2}{\pi} \lambda E_1. \tag{13}$$

At low energies, $E_1 \ll \varepsilon_2$, the symmetric amplitude again leads to $\beta = 2$:

$$\Gamma^{+}_{1,2,3}(E_1) \simeq \lambda \frac{E_1^2}{2\varepsilon_2}. \tag{14}$$

However, for the antisymmetric amplitude, destructive interference effects result in $\beta = 3$ in the low-energy limit, $E_1 \ll \varepsilon_2$:

$$\Gamma^{-}_{1,2,3}(E_1) \simeq \frac{3\pi - 8}{24\pi} \lambda \frac{E_1^3}{\varepsilon_2^2}. \tag{15}$$

Figure 3 depicts the decay width $\Gamma_{1,2,3}(E_1)$ as a function of E_1 for these scenarios, including the one-body decay width $\Gamma_{12}(E_1)$ to emphasize the relative longevity of configurations involving two s-wave neutrons. This observation supports arguments in Ref. [26]: the s-wave two-body decay width in the experimentally relevant energy range is close to the simple law $\Gamma \simeq E$. The variations in the phase-space energy scaling discussed herein arise from the quantum evolution through an intermediate state. Earlier discussions on similar phenomena are available in Refs. [3,26–28] (Figs. 3 and 4).

The two-nucleon decay is clearly a very rich subject where many types of behaviors are possible that offer a lot of experimental roads for studying the quantum evolution of wave functions; some possibilities are discussed in Ref. [2].

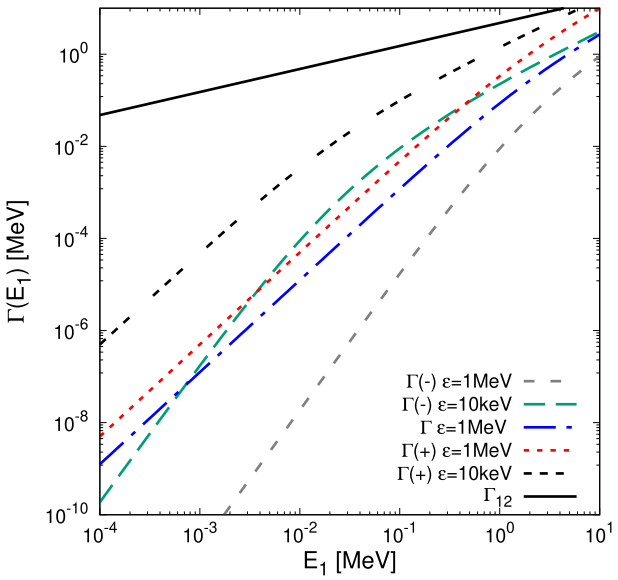

Fig. 3 This figure illustrates the energy dependence of decay widths, plotting $\Gamma^{\pm}_{1,2,3}(E_1)$ for identical particles (denoted as $\Gamma(+)$ for symmetric and $\Gamma(-)$ for antisymmetric combinations) alongside $\Gamma_{1,2,3}(E_1)$ for distinguishable particles (represented as Γ), against the total decay energy E_1. Additionally, the one-body decay width $\Gamma_{1,2}(E_1)$ as a function of energy is shown for comparison. The parameter ε_2, indicating the energy levels of interest, is specified for each curve

3 Near-Threshold Physics

The near-threshold physics has a long history [29–35]. The interaction with continuum introduces an additional effective Hamiltonian H' in the internal space Q as described by the following integral expression [8,15]:

$$H'(\epsilon) = \int_0^\infty d\epsilon' \frac{|A(\epsilon')|^2}{\epsilon - \epsilon' + i0}. \tag{16}$$

In this context, we adopt an on-shell approximation applicable under the assumption that the internal and continuum spaces are orthogonal. The comprehensive formulation and its derivation were detailed in Refs. [8, 15].

For simplicity, in a single-channel scenario, we omit the subscripts using $A_{1,2} \equiv A$ and reference all energies from the channel threshold denoted by $E = \epsilon$. The interaction term in eq. (16) reflects the second-order effect resulting from excitations in the continuum. Unlike perturbation theory, the Feshbach projection formalism provides an exact solution. The precise eigenvalues in the full space are determined from the energy-dependent Hamiltonian $\mathcal{H}(E) = H_{QQ} + H'(E)$ employing a nonlinear variant of the Schrödinger equation,

$$\mathcal{H}(E)|I\rangle = E|I\rangle. \tag{17}$$

Typically, both H' and $\mathcal{H}$ appear as non-Hermitian operators.

When a decay channel satisfies $\epsilon > 0$, the integration in eq. (16) encounters a pole, necessitating the division of the integral into a Hermitian principal value component, $\Delta(\epsilon)$, representing the self-energy, and a non-Hermitian segment, $\Gamma(\epsilon)$, indicating the decay width,

$$H'(\epsilon) = \Delta(\epsilon) - \frac{i}{2}\Gamma(\epsilon), \tag{18}$$

$$\Delta(\epsilon) = \mathcal{P}\int d\epsilon' \frac{|A(\epsilon')|^2}{\epsilon - \epsilon'}, \tag{19}$$

$$\Gamma(\epsilon) = 2\pi|A(\epsilon)|^2. \tag{20}$$

Here, $\mathcal{P}$ denotes the Cauchy principal value of the integral, ensuring the separation of Hermitian and non-Hermitian contributions to the effective Hamiltonian.

The significance of the non-Hermitian component Γ within the context of the nuclear many-body problem is thoroughly examined in Refs. [8,15]. This term is distinguished by its factorized structure that is instrumental in preserving the unitarity of the scattering matrix. The inherent factorization of Γ facilitates a dynamical phase transition often referred to as *superradiance*, a phenomenon that is discussed in Refs. [14,16,36] and further elaborated in Sect. 5.

Additionally, the Hermitian correction attributed to virtual excitations into continuum and denoted by $\Delta(\epsilon)$, plays a crucial role in adjusting the positions of both bound and resonant states in proximity of decay thresholds. These adjustments can lead to pronounced variations in spectroscopic observables as systems approach their decay thresholds, a topic that has been explored in detail in Ref. [37]. Such studies reveal the intricate interplay between the Hermitian and non-Hermitian components in shaping the nuclear landscape, particularly in regions near decay thresholds where quantum phenomena such as superradiance and phase transitions become prominent.

4 Exotic Decay of ^{11}Be

Here we discuss an example of ^{11}Be sequential decay, which is not fully understood yet but clearly highlights some important physics related to decay and threshold phenomena discussed in this work. The persistent discrepancy in neutron lifetime measurements observed through two different experimental approaches, as highlighted in Ref. [38], has sparked a range of speculative theories. Among these, especially intriguing is the hypothesis that this variance might stem from an unaccounted neutron decay into unobserved dark matter particles. This possibility was scrutinized in Ref. [39] that also explores the feasibility of investigating such a decay channel via alternative nuclear beta decays.

In this context, the nucleus ^{11}Be emerges as a prime candidate for further studies. Characterized by its composition of four protons and seven neutrons, ^{11}Be is distinguished as a neutron halo nucleus. Its structural peculiarities are noteworthy: while six neutrons fill the lowest $0s_{1/2}$ and $0p_{3/2}$ levels within the mean-field potential, an additional halo neutron occupies the $1s_{1/2}$ level positioned merely 320 keV below the $0p_{1/2}$ state. This deviation from the conventional shell structure, a threshold effect, is attributed to the pronounced coupling between the s-orbit and the continuum, as argued in Refs. [21,40,41]. Such coupling, being facilitated by virtual excitations, eq. (19), is believed to lower the energy level of the s-orbit, thereby altering the expected shell configuration.

The beta decay width as a function of decay energy is given by the combination of Fermi and Gamow-Teller transitions,

$$\gamma_\beta(\epsilon) = \frac{\ln 2}{t} = \frac{f(\epsilon)\,\hbar\,\ln 2}{\mathcal{T}}\left(B(F) + \lambda_A^2 B(GT)\right), \tag{21}$$

here t is half-life, $\mathcal{T}$ and λ_A are constants, $B(F)$ and $B(GT)$ are nuclear matrix elements. The energy dependence is given by the phase space volume $f(\epsilon)$ that typically increases rapidly with energy often following a power law as discussed earlier. This rapid increase means that the decay rates are highly sensitive to the decay energies, the Q-values.

For the beta decay of ^{11}Be,

$$^{11}\mathrm{Be} \rightarrow {}^{11}\mathrm{B} + e^- + \bar{\nu}_e, \tag{22}$$

an energy release of 11.5092 MeV is observed; it is large primarily because a proton is strongly bound within ^{11}B. This significant release of energy leads to a notably shorter half-life for ^{11}Be, estimated as $t_{\mathrm{Be}} = 13.6 \pm 0.07$ seconds. In contrast, the Q-value for potential decay into dark matter is reduced by the neutron separation energy. Through a phase space analysis, it is possible to infer a lower limit for the half-life associated with the dark matter decay from ^{11}Be, as $t_{\mathrm{Be}\rightarrow X} > 10^5$ seconds [39].

For a conventional explanation, the authors of Ref. [42] propose the presence of a resonance in ^{11}B, located 196 keV above the proton decay threshold. Analyzing the experimental distribution of proton energies, they deduce the proton resonance width to be $\Gamma = 12(5)$ keV. Furthermore, they propose a $\log_{10}(ft)$ value of 4.8(4) for the beta decay transition into this specific resonance. This resonance has been recently confirmed experimentally [43,44]. The notable positioning of a strong resonance just near threshold, which seems "convenient," may not be coincidental. Instead, it is likely a consequence of the resonant attraction phenomena explored in Sect. 3, as further detailed in [45].

The assessment of the beta decay strength is conventionally performed using the ft value, as

$$ft = \frac{\mathcal{T}}{B(F) + \lambda_A^2 B(GT)}. \tag{23}$$

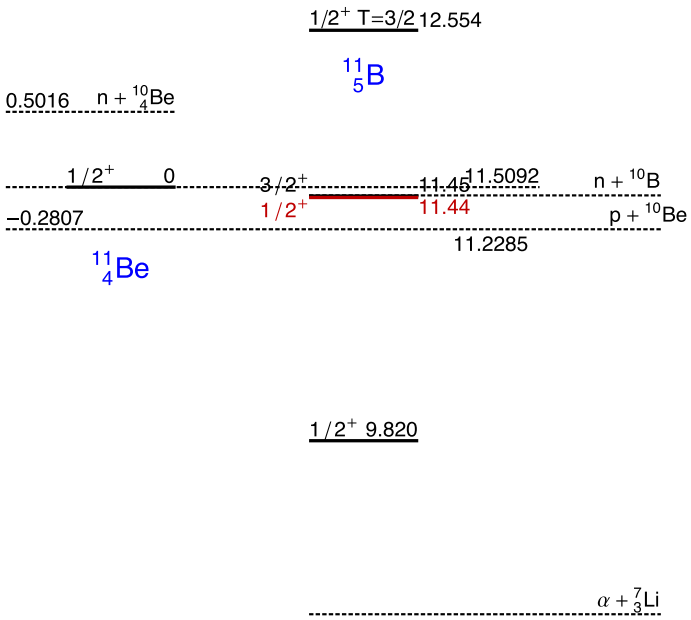

Fig. 4 Schematic figure showing the level scheme of ^{11}Be along with all of the relevant thresholds. The position of the newly observed resonance is highlighted in red

Setting $E_1 = 0$ and defining Q as the negative of E_3, we can analogously express the integrated width for sequential decay, following our discussion in Sect. 2, through a similar formula,

$$\mathcal{F}t = \frac{\mathcal{T}}{B(F) + \lambda^2 B(GT)}, \tag{24}$$

that incorporates an effective energy-dependent function

$$\mathcal{F}(Q) = \int_0^Q \frac{d\epsilon}{2\pi} \frac{f(\epsilon)\Gamma_2(Q-\epsilon)}{(\epsilon + E_2)^2 + \Gamma_2^2(Q-\epsilon)/2}. \tag{25}$$

In scenarios where the intermediate state E_2 is below zero indicating an open sequential decay channel, the integral in eq. (25) encounters a pole. In cases where Γ_2 is negligibly small, $\mathcal{F}(Q)$ simplifies to $f(Q)$, thus reverting to the classical limit, just as was illustrated in Fig. 1.

For the purpose of analyzing eq. (24), and following [46], we adopt $t \equiv t_{\mathrm{Be}\to\beta p} = 1 \times 10^6$ s, as suggested by experimental data. The analysis in Fig. 5 explores the variation of $\log_{10}(\mathcal{F}t)$ focusing on the influence of the intermediate proton resonance position E_2. We remind that $Q = 0.2807$ MeV and energy of the initial state $E_1 = 0$, so for $E_2 > 0$ the decay is virtual. We take the decay width on an intermediate resonance $\Gamma_2(\epsilon)$ as a sum of the proton decay width $\gamma_p(\epsilon)$ and a constant alpha decay width γ_α:

$$\Gamma_2(\epsilon) = \gamma_p(\epsilon) + \gamma_\alpha, \tag{26}$$

with γ_α presumed to be constant because alpha decay threshold is far away. We employ a potential model to obtain the energy dependent proton decay width. We estimate the alpha decay width to be in the range from 1 keV to 200 keV [46]. For a reference, the $3/2^+_2$ state at 9.873 MeV excitation is known to possess an alpha decay width of 109 keV, Ref. [46,47].

Figure 5 can be viewed as describing conditions needed to explain the $t \equiv t_{\mathrm{Be}\to\beta p} = 1 \times 10^6$ second half-life, one is the position of an intermediate proton resonance (x-axis) and the second one is the strength of the initial beta decay described by the Gamow-Teller matrix element $\log_{10}(ft)$ on the y-axis. The presence of an open alpha decay channel is making the observed half-life more difficult to explain as a significant fraction of decays is expected to proceed along the alpha channel (beta-delayed alpha decay) and not lead to a final ^{10}Be. Thus curves (c) and (d) in Fig. 5 show lower $\log_{10}(ft)$. Figure 5 shows that given the experimentally observed position of the resonance the data would be explained if $\log_{10}(ft)$ is between 2 and 3.

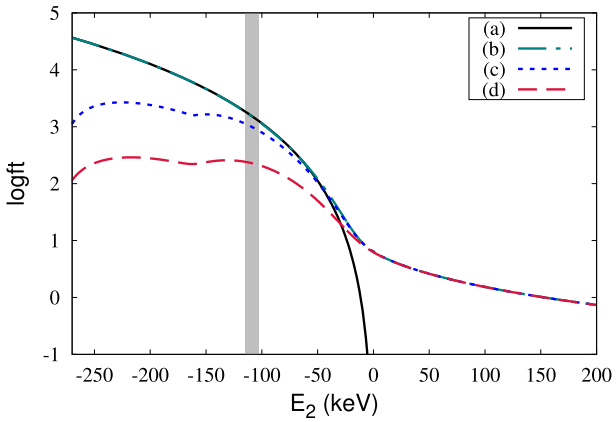

Fig. 5 The $\log_{10}(\mathcal{F}t)$ value for fixed $t \equiv t_{^{11}\mathrm{Be}\to\beta p} = 1 \times 10^6$ is shown as a function of E_2 which is the energy of the proton resonance in ^{11}B, relative to the beta decay threshold. The figure includes the following curves: **a** Classical beta decay $\log_{10}(ft)$ for ^{11}Be decaying to ^{11}B. **b** Effective $\log_{10}(\mathcal{F}t)$ for beta-delayed proton emission going through a resonant state in ^{11}B, eq. (24), with $\mathrm{SF}_p = 0.23$ and $\gamma_\alpha = 0$. **c** Same as **b** but with $\gamma_\alpha = 1$ keV. **d** Same as **b** and **c** but with $\gamma_\alpha = 10$ keV. The position of the state and its width suggested by the experimental data are shown by the shaded area

Table 1 Theoretical and experimental data for $1/2^+$ states that can serve as potential intermediate states in the beta-delayed proton decay process

J_i^π	Theory			Experiment	
	E(MeV)	log(ft)	SF(p)	E(MeV)	SF(p)
$1/2^+_1$	5.709	5.5	0.262	6.792	
$1/2^+_2$	10.545	3.4	0.117	9.820	
$1/2^+_3$	11.952	3.5	0.134	11.44	0.27(6)
$1/2^+_4$ T=3/2	12.181		0.274	12.554	
$1/2^+_5$	12.827	4.0	0.028		
$1/2^+_6$	14.105	5.4	0.001		

The shell model analysis with the FSU Hamiltonian [48] is presented in Table 1 along with available experimental data, only states $1/2^+$ are included which are relevant here. The table includes the $\log_{10}(ft)$. All states have $\log_{10}(ft)$ above 3.5 which is rather typical indicating about a factor of 10 discrepancy with analysis in Fig. 5. Note that $\log_{10}(ft) \approx 4.8$ was suggested in Ref. [42].

Currently, a substantial amount of theoretical research exists [49–52] that provides insight into the "convenient" positioning of the resonance and its proton strength. In particular, the reasons behind the position of the proton resonance, its attraction to the threshold, lack of alpha decay and strong proton decay may follow from the near-threshold physics discussed in Sect. 3. On the other hand, it is unclear why, despite the low Q-value, the beta decay rate surpasses the predictions of conventional theories.

The double beta decay, is another related process [53] (we do not even go here into the discussion of the neutrinoless one) which is of the second order virtual type with typical halflifes of 10^{19} years or longer, exceeding the age the universe by many orders of magnitude [54,55]. These decays probe the extreme tail of the virtual process Fig. 1 with power-law phase-space scaling parameter β being approximately between 9 and 11. The physics of the process and even the systematics of the lifetimes is far from being fully understood.

5 Decay and Overlapping Resonances

This presentation would not be complete without mentioning the decay process with interference of resonances. There physics can be described using the non-Hermitian effective Hamiltonian approach mentioned in Sect. 3 that leads to a number of remarkable phenomena, such as superradiance [56] recently observed in alpha decays [57], interference of resonances such as those in ^{13}C, near-threshold effects [58], statistical properties of the decay width distribution [59], interplay with giant resonances [60] and emergence of the pygmy dipole

strength [61], bound states in the continuum [62], transport phenomena, etc. [13]. The simplest two-level model provides a very nice and minimal picture highlighting the phenomena [63].

Consider two quantum states (*1* and *2*) with energies ϵ_1 and ϵ_2. Their independent decay amplitudes A_1 and A_2 define their decay widths following eq. (2); for brevity we take $\gamma = A^2$, where the amplitudes are real. The states interact through the Hermitian operator, resulting in an off-diagonal matrix element V. This brings us to the simplest model characterized by the 2×2 effective non-Hermitian Hamiltonian,

$$\mathcal{H} = \begin{pmatrix} \epsilon_1 - (i/2)A_1^2 & V - (i/2)A_1A_2 \\ V - (i/2)A_1A_2 & \epsilon_2 - (i/2)A_2^2 \end{pmatrix}. \tag{27}$$

The diagonalization of this Hamiltonian provides two decaying states with complex energies

$$\mathcal{E}_\pm = \bar{\mathcal{E}} \pm \frac{1}{2}\sqrt{X - iY}, \tag{28}$$

where

$$\bar{\mathcal{E}} = \frac{1}{2}[\epsilon_1 + \epsilon_2 - (i/2)(\gamma_1 + \gamma_2)], \tag{29}$$

and

$$X = (\epsilon_1 - \epsilon_2)^2 + 4V^2 - \frac{1}{4}(\gamma_1 + \gamma_2)^2, \tag{30}$$

$$Y = (\epsilon_1 - \epsilon_2)(\gamma_1 - \gamma_2) + 4VA_1A_2. \tag{31}$$

Separating real and imaginary parts

$$\mathcal{E}_\pm = E_\pm - \frac{i}{2}\Gamma_\pm, \tag{32}$$

we get the resonance energies and widths.

Unlike the situation with stationary states, partial level crossing is possible when $Y = 0$, then depending on the sign of X we have either crossing of real energies or widths, a full crossing is also possible when both X and Y are zero, see the discussion in [63] and references therein. The stationary state in the continuum emerges when

$$V(\gamma_1 - \gamma_2) = A_1A_2(\epsilon_1 - \epsilon_2). \tag{33}$$

When real part of the effective hamiltonian is large and we can neglect the terms of the second order in $\gamma_{1,2}$ in eq. (30) resulting in the standard Wigner repulsion for bound states

$$E_\pm = \frac{1}{2}[\epsilon_1 + \epsilon_2 \pm \sqrt{(\epsilon_1 - \epsilon_2)^2 + 4V^2}], \tag{34}$$

and

$$\Gamma_\pm = \frac{1}{2}\left(\gamma_1 + \gamma_2 \pm \frac{(\epsilon_1 - \epsilon_2)(\gamma_1 - \gamma_2) + 4VA_1A_2}{\sqrt{(\epsilon_1 - \epsilon_2)^2 + 4V^2}}\right). \tag{35}$$

For the large level separation or small V, we come to the trivial result with the widths $\Gamma_\pm$ being reduced to $\gamma_{1,2}$, with the exception of an interesting competing limit $\gamma_1 = \gamma_2$ in which case the decay drives the mixing of the states. Another interesting limit is when $\epsilon_1 \approx \epsilon_2$, while V remains large, then $\Gamma_\pm = \frac{1}{2}(A_1 \pm A_2)^2$ that displays the separation of widths into large and small ones.

In Fig. 6 we show typical dynamics of complex poles in the complex plane as coupling to the continuum increases. Here we increase A_1 keeping all other parameters fixed. The picture is quite generic: one state always returns to the real axis becoming effectively bound, while the other state absorbs the entire width and becomes superradiant. This superradiance mechanism is central for many remarkable phenomena providing a potential explanation for the presence and structure of the proton resonant state in ^{11}Be discussed earlier.

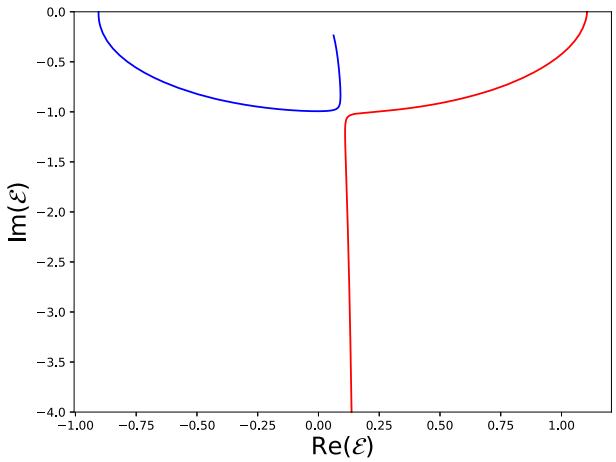

Fig. 6 Dynamics of two complex resonances (poles in the scattering matrix) for a two state model (27). The parameter choice here is: $\epsilon_1 = 0.2$, $\epsilon_2 = 0$, $A2 = -0.099$, and $V = 1$; the A_1 is varied

6 Conclusion

In this brief presentation we went through few remarkable examples and puzzles of the quantum dynamics for nuclear systems displaying the complex interplay of internal fermionic dynamics, continuum effects, radioactive decays, relaxation of many-body states, quantum resonances of various nature, threshold phenomena, superradiance, effects of quantum complexity and peculiarities of specific quantum states. This is a broad area of studies with broad applications not only in the nuclear physics but also for astrophysics and general many-body quantum physics.

Acknowledgements This material is based upon work supported by the US Department of Energy Office of Science, Office of Nuclear Physics under Award No. DE-SC0009883. V.Z. is grateful to B. Pritychenko for the discussion of double beta decay and corresponding data.

Author contribution The authors contributed equally to the research work reported.

Data Availability No datasets were generated or analysed during the current study.

Declarations

Conflict of interest The authors declare no competing interests.

References

1. M. Peshkin, A. Volya, V. Zelevinsky, Non-exponential and oscillatory decays in quantum mechanics. EPL **107**(4), 40001 (2014)
2. S.M. Wang, W. Nazarewicz, A. Volya, Y.G. Ma, Probing the nonexponential decay regime in open quantum systems. Phys. Rev. Res. **5**(2), 023183 (2023). https://doi.org/10.1103/PhysRevResearch.5.023183
3. A. Spyrou, Z. Kohley, T. Baumann, D. Bazin, B.A. Brown, G. Christian, P.A. DeYoung, J.E. Finck, N. Frank, E. Lunderberg, S. Mosby, W.A. Peters, A. Schiller, J.K. Smith, J. Snyder, M.J. Strongman, M. Thoennessen, A. Volya, First observation of ground state dineutron decay: ^{16}Be. Phys. Rev. Lett. **108**(10), 102501 (2012)
4. C.R. Hoffman, T. Baumann, J. Brown, P.A. DeYoung, J.E. Finck, N. Frank, J.D. Hinnefeld, S. Mosby, W.A. Peters, W.F. Rogers, A. Schiller, J. Snyder, A. Spyrou, S.L. Tabor, M. Thoennessen, Observation of a two-neutron cascade from a resonance in ^{24}O. Phys. Rev. C **83**(3), 031303 (2011). https://doi.org/10.1103/PhysRevC.83.031303
5. E. Lunderberg, P.A. DeYoung, Z. Kohley, H. Attanayake, T. Baumann, D. Bazin, G. Christian, D. Divaratne, S.M. Grimes, A. Haagsma, J.E. Finck, N. Frank, B. Luther, S. Mosby, T. Nagi, G.F. Peaslee, A. Schiller, J. Snyder, A. Spyrou, M.J. Strongman, M. Thoennessen, Evidence for the ground-state resonance of ^{26}O. Phys. Rev. Lett. **108**(14), 142503 (2012). https://doi.org/10.1103/PhysRevLett.108.142503
6. H.T. Johansson, Y. Aksyutina, T. Aumann, K. Boretzky, M.J.G. Borge, A. Chatillon, L.V. Chulkov, D. Cortina-Gil, U.D. Pramanik, H. Emling, C. Forssen, H.O.U. Fynbo, H. Geissel, G. Ickert, B. Jonson, R. Kulessa, C. Langer, M. Lantz, T. LeBleis, K. Mahata, M. Meister, G. Muenzenberg, T. Nilsson, G. Nyman, R. Palit, S. Paschalis, W. Prokopowicz, R. Reifarth, A.

Richter, K. Riisager, G. Schrieder, N.B. Shulgina, H. Simon, K. Suemmerer, O. Tengblad, H. Weick, M.V. Zhukov, Three-body correlations in the decay of ^{10}He and ^{13}Li. Nucl. Phys. A. (2010). https://doi.org/10.1016/j.nuclphysa.2010.07.002
7. N. Michel, W. Nazarewicz, M. Ploszajczak, J. Okolowicz, Gamow shell model description of weakly bound nuclei and unbound nuclear states. Phys. Rev. C **67**, 054311 (2003)
8. A. Volya, V. Zelevinsky, Collective dipole excitations in the continuum shell model. Phys. Scr. **T125**(T125), 224–225 (2006)
9. T. Myo, K. Kato, K. Ikeda, Resonances of ^{7}He using the complex scaling method. Phys. Rev. C **76**(5), 054309 (2007). https://doi.org/10.1103/PhysRevC.76.054309
10. L.V. Grigorenko, I.G. Mukha, C. Scheidenberger, M.V. Zhukov, Two-neutron radioactivity and four-nucleon emission from exotic nuclei. Phys. Rev. C **84**(2), 021303 (2011). https://doi.org/10.1103/PhysRevC.84.021303
11. H. Feshbach, The optical model and its justification. Annu. Rev. Nucl. Sci. **8**, 49 (1958)
12. H. Feshbach, A unified theory of nuclear reactions. Ann. Phys. **19**, 287 (1962)
13. V. Zelevinsky, A. Volya, *Mesoscopic nuclear physics: from nucleus to quantum chaos to quantum signal transmission* (World Scientific, Singapore, 2023). https://doi.org/10.1142/13049
14. V.V. Sokolov, V.G. Zelevinsky, Dynamics and statistics of unstable quantum states. Nucl. Phys. A **504**, 562 (1989)
15. A. Volya, Time-dependent approach to the continuum shell model. Phys. Rev. C **79**(4), 044308 (2009). https://doi.org/10.1103/PhysRevC.79.044308
16. N. Auerbach, V. Zelevinsky, Super-radiant dynamics, doorways and resonances in nuclei and other open mesoscopic systems. Rep. Prog. Phys. **74**, 106301 (2011). https://doi.org/10.1088/0034-4885/74/10/106301
17. Y. Kondo, T. Nakamura, R. Tanaka, R. Minakata, S. Ogoshi, N.A. Orr, N.L. Achouri, T. Aumann, H. Baba, F. Delaunay, P. Doornenbal, N. Fukuda, J. Gibelin, J.W. Hwang, N. Inabe, T. Isobe, D. Kameda, D. Kanno, S. Kim, N. Kobayashi, T. Kobayashi, T. Kubo, S. Leblond, J. Lee, F.M. Marqués, T. Motobayashi, D. Murai, T. Murakami, K. Muto, T. Nakashima, N. Nakatsuka, A. Navin, S. Nishi, H. Otsu, H. Sato, Y. Satou, Y. Shimizu, H. Suzuki, K. Takahashi, H. Takeda, S. Takeuchi, Y. Togano, A.G. Tuff, M. Vandebrouck, K. Yoneda, Nucleus ^{26}O: a barely unbound system beyond the drip line. Phys. Rev. Lett. **116**, 102503 (2016). https://doi.org/10.1103/PhysRevLett.116.102503
18. Z. Kohley, E. Lunderberg, P.A. DeYoung, A. Volya, T. Baumann, D. Bazin, G. Christian, N.L. Cooper, N. Frank, A. Gade, C. Hall, J. Hinnefeld, B. Luther, S. Mosby, W.A. Peters, J.K. Smith, J. Snyder, A. Spyrou, M. Thoennessen, First observation of the ^{13}Li ground state. Phys. Rev. C **87**(1), 011304 (2013)
19. R.J. Charity, J. Wylie, S.M. Wang, T.B. Webb, K.W. Brown, G. Cerizza, Z. Chajecki, J.M. Elson, J. Estee, D.E.M. Hoff, S.A. Kuvin, W.G. Lynch, J. Manfredi, N. Michel, D.G. McNeel, P. Morfouace, W. Nazarewicz, C.D. Pruitt, C. Santamaria, S. Sweany, J. Smith, L.G. Sobotka, M.B. Tsang, A.H. Wuosmaa, Strong evidence for ^{9}N and the limits of existence of atomic nuclei. Phys. Rev. Lett. **131**, 172501 (2023). https://doi.org/10.1103/PhysRevLett.131.172501
20. I.A. Egorova, R.J. Charity, L.V. Grigorenko, Z. Chajecki, D. Coupland, J.M. Elson, T.K. Ghosh, M.E. Howard, H. Iwasaki, M. Kilburn, J. Lee, W.G. Lynch, J. Manfredi, S.T. Marley, A. Sanetullaev, R. Shane, D.V. Shetty, L.G. Sobotka, M.B. Tsang, J. Winkelbauer, A.H. Wuosmaa, M. Youngs, M.V. Zhukov, Democratic decay of ^{6}Be exposed by correlations. Phys. Rev. Lett. **109**, 202502 (2012). https://doi.org/10.1103/PhysRevLett.109.202502
21. A. Volya, Physics of unstable nuclei: from structure to sequential decays. EPJ Web of Conf. **38**, 03003 (2012)
22. Baz, A.I., Zeldovich, I.B., Perelomov, A.M.: Scattering, Reactions and Decay in Nonrelativistic Quantum Mechanics, (1971)
23. L.D. Landau, E.M. Lifshitz, *Quantum Mechanics Non-relativistic Theory*, 3rd edn. (Pergamon Press, New York, 1981)
24. N. Michel, M. Płoszajczak, *Gamow Shell Model, The Unified Theory of Nuclear Structure and Reactions*, Lecture Notes in Physics, vol. 983. (Springer, Switzerland, 2021)
25. A. Bohr, B.R. Mottelson, *Nuclear Structure* (World Scientific Publishing, Singapore, 1998)
26. L.V. Grigorenko, M.V. Zhukov, Problems with the interpretation of the (10)he ground state. Phys. Rev. C **77**(3), 034611 (2008). https://doi.org/10.1103/PhysRevC.77.034611
27. S.E. Koonin, Proton pictures of high-energy nuclear collisions. Phys. Lett. B (1977). https://doi.org/10.1016/0370-2693(77)90340-9
28. R. Lednicky, V.L. Lyuboshits, Effect of the final-state interaction on pairing correlations of particles with small relative momenta. Sov. J. Nucl. Phys. **35**, 5 (1982)
29. E.P. Wigner, On the behavior of cross sections near thresholds. Phys. Rev. **73**(9), 1002–1009 (1948). https://doi.org/10.1103/PhysRev.73.1002
30. F.C. Barker, A model for nuclear threshold levels. Proc. Phys. Soc. **84**(5), 681 (1964). https://doi.org/10.1088/0370-1328/84/5/305
31. D.R. Inglis, Nuclear models, threshold states and rearrangement energy. Nucl. Phys. **30**, 1–29 (1962). https://doi.org/10.1016/0029-5582(62)90029-9
32. A.I. Baz', Energy dependence of cross sections near the "threshold" for unstable particle production. JETP **13**(5), 1058 (1961)
33. A.I. Baz', Resonance effects in the scattering of particles near a reaction threshold. JETP **9**(6), 1256 (1959)
34. A.I. Baz', The energy dependence of a scattering cross section near the threshold of reaction. JETP **6**(4), 709 (1958)
35. G. Breit, Energy dependence of reactions at thresholds. Phys. Rev. **107**(6), 1612–1615 (1957). https://doi.org/10.1103/PhysRev.107.1612
36. I. Rotter, A non-hermitian hamilton operator and the physics of open quantum systems. J. Phys. Al **42**(15), 153001 (2009). https://doi.org/10.1088/1751-8113/42/15/153001
37. N. Michel, W. Nazarewicz, M. Ploszajczak, T. Vertse, Shell model in the complex energy plane. J. Phys. G **36**(1), 013101 (2009). https://doi.org/10.1088/0954-3899/36/1/013101
38. F.E. Wietfeldt, G.L. Greene, Colloquium: the neutron lifetime. Rev. Mod. Phys. **83**, 1173–1192 (2011). https://doi.org/10.1103/RevModPhys.83.1173
39. M. Pfützner, K. Riisager, Examining the possibility to observe neutron dark decay in nuclei. Phys. Rev. C **97**, 042501 (2018). https://doi.org/10.1103/PhysRevC.97.042501

40. A. Volya, V. Zelevinsky, Exploring dynamics of unstable many-body systems. AIP Conf. Proc. **1619**, 181–189 (2014). https://doi.org/10.1063/1.4899234
41. C.R. Hoffman, B.P. Kay, J.P. Schiffer, Neutron s states in loosely bound nuclei. Phys. Rev. C **89**, 061305 (2014). https://doi.org/10.1103/PhysRevC.89.061305
42. Y. Ayyad, B. Olaizola, W. Mittig, G. Potel, V. Zelevinsky, M. Horoi, S. Beceiro-Novo, M. Alcorta, C. Andreoiu, T. Ahn, M. Anholm, L. Atar, A. Babu, D. Bazin, N. Bernier, S.S. Bhattacharjee, M. Bowry, R. Caballero-Folch, M. Cortesi, C. Dalitz, E. Dunling, A.B. Garnsworthy, M. Holl, B. Kootte, K.G. Leach, J.S. Randhawa, Y. Saito, C. Santamaria, P. Siuryte, C.E. Svensson, R. Umashankar, N. Watwood, D. Yates, Direct observation of proton emission in ^{11}Be. Phys. Rev. Lett. **123**, 082501 (2019). https://doi.org/10.1103/PhysRevLett.123.082501
43. Y. Ayyad, W. Mittig, T. Tang, B. Olaizola, G. Potel, N. Rijal, N. Watwood, H. Alvarez-Pol, D. Bazin, M. Caamaño, J. Chen, M. Cortesi, B. Fernández-Domínguez, S. Giraud, P. Gueye, S. Heinitz, R. Jain, B.P. Kay, E.A. Maugeri, B. Monteagudo, F. Ndayisabye, S.N. Paneru, J. Pereira, E. Rubino, C. Santamaria, D. Schumann, J. Surbrook, L. Wagner, J.C. Zamora, V. Zelevinsky, Evidence of a near-threshold resonance in ^{11}B relevant to the β-delayed proton emission of ^{11}Be. Phys. Rev. Lett. **129**, 012501 (2022). https://doi.org/10.1103/PhysRevLett.129.012501
44. E. Lopez-Saavedra, S. Almaraz-Calderon, B.W. Asher, L.T. Baby, N. Gerken, K. Hanselman, K.W. Kemper, A.N. Kuchera, A.B. Morelock, J.F. Perello, E.S. Temanson, A. Volya, I. Wiedenhöver, Observation of a near-threshold proton resonance in ^{11}B. Phys. Rev. Lett. **129**, 012502 (2022). https://doi.org/10.1103/PhysRevLett.129.012502
45. J. Okołowicz, M. Płoszajczak, W. Nazarewicz, Convenient location of a near-threshold proton-emitting resonance in ^{11}B. Phys. Rev. Lett. **124**, 042502 (2020). https://doi.org/10.1103/PhysRevLett.124.042502
46. A. Volya, Assessment of the beta-delayed proton decay rate of 11Be. EPL **130**(1), 12001 (2020). https://doi.org/10.1209/0295-5075/130/12001
47. J. Refsgaard, J. Büscher, A. Arokiaraj, H.O.U. Fynbo, R. Raabe, K. Riisager, Clarification of large-strength transitions in the β decay of ^{11}Be. Phys. Rev. C **99**, 044316 (2019). https://doi.org/10.1103/PhysRevC.99.044316
48. R.S. Lubna, K. Kravvaris, S.L. Tabor, V. Tripathi, E. Rubino, A. Volya, Evolution of the N=20 and 28 shell gaps and two-particle-two-hole states in the FSU interaction. Phys. Rev. Res. **2**(4), 043342 (2020). https://doi.org/10.1103/PhysRevResearch.2.043342
49. M.C. Atkinson, P. Navrátil, G. Hupin, K. Kravvaris, S. Quaglioni, Ab initio calculation of the β decay from ^{11}Be to a ^{10}Be$+p$ resonance. Phys. Rev. C **105**, 054316 (2022). https://doi.org/10.1103/PhysRevC.105.054316
50. J. Okołowicz, M. Płoszajczak, W. Nazarewicz, $\beta-$p and $\beta-\alpha$ decay of the ^{11}Be neutron halo ground state. J. Phys G **49**(10), 10–01 (2022). https://doi.org/10.1088/1361-6471/ac8948
51. N. Le Anh, B.M. Loc, N. Auerbach, V. Zelevinsky, Single-particle properties of the near-threshold proton-emitting resonance in ^{11}Be. Phys. Rev. C **106**(5), 051302 (2022). https://doi.org/10.1103/PhysRevC.106.L051302
52. W. Elkamhawy, Z. Yang, H.-W. Hammer, L. Platter, β-delayed proton emission from 11be in effective field theory. Phys. Lett. B **821**, 136610 (2021). https://doi.org/10.1016/j.physletb.2021.136610
53. T. Tomoda, Double beta decay. Rep. Prog. Phys. **54**(1), 53 (1991). https://doi.org/10.1088/0034-4885/54/1/002
54. H. Primakoff, S.P. Rosen, Double beta decay. Rep. Prog. Phys. **22**(1), 121 (1959). https://doi.org/10.1088/0034-4885/22/1/305
55. B. Pritychenko, Systematic analysis of double-beta decay half lives. Nucl. Phys. A **1033**, 122628 (2023). https://doi.org/10.1016/j.nuclphysa.2023.122628
56. N. Auerbach, V. Zelevinsky, Super-radiant dynamics, doorways and resonances in nuclei and other open mesoscopic systems. Rep. Prog. Phys. **74**, 106301 (2011)
57. A. Volya, M. Barbui, V.Z. Goldberg, G.V. Rogachev, Superradiance in alpha clustered mirror nuclei. Commun. Phys. **5**(1), 1–6 (2022). https://doi.org/10.1038/s42005-022-01105-9
58. A. Volya, V. Zelevinsky, Continuum shell model. Phys. Rev. C **74**(6), 064314 (2006)
59. A. Volya, Porter-thomas distribution in unstable many-body systems. Phys. Rev. C **83**(4), 044312 (2011)
60. C.H. Lewenkopf, V.G. Zelevinsky, Single and multiple giant-resonances - counterplay of collective and chaotic dynamics. Nucl. Phys. A **569**(1–2), 194 (1994)
61. A. Volya, V. Zelevinsky, Collective many-body dynamics in the vicinity of nuclear driplines. Nucl. Phys. A **788**, 251 (2007)
62. N. Auerbach, V. Zelevinsky, A. Volya, "Super-radiance" and the width of exotic baryons. Phys. Lett. B **590**(1–2), 45–50 (2004)
63. A. Volya, V. Zelevinsky, Non-hermitian effective hamiltonian and continuum shell model. Phys. Rev. C **67**(5), 054322 (2003)